2005

Mapping Near-Surface Gas with Acoustic Remote Sensing Methods, Examples from Eel River Margin, CA and Skjalfandi Bay, Iceland

Luciano E. Fonseca
University of New Hampshire, Durham, luciano@ccom.unh.edu

Larry A. Mayer
University of New Hampshire, larry.mayer@unh.edu

Mapping Near-Surface Gas with Acoustic Remote Sensing Methods, Examples from Eel River Margin, CA and Skjalfandi Bay, Iceland

Luciano Fonseca[1], Larry Mayer[2]

Abstract

Acoustic remote sensing systems such as multibeam and sidescan sonars can be used for mapping and detection of near-surface gas in marine sediments. These systems can provide a realistic depiction of the seafloor by means of the simultaneous acquisition of co-registered high-resolution bathymetry and calibrated seafloor backscatter. An acoustical backscattering model for gassy sediments is used to recognize gas signature in multibeam sonar records. Additionally, analysis of backscatter images and detailed bathymetry reveals anomalous seafloor features, which are associated with gas expulsion. These processed acoustic remote sensing data can be interpreted in conjunction with other geological, geophysical and geochemical data from an exploration area, to help explain the distribution and origin of near-surface gas. The Eel River Basin offshore Northern California will be used to assess the applicability of acoustic remote sensing methods for the location of near-surface gas accumulations. In this area, an immense database of marine information was collected, including acoustic remote sensing data collected at 95kHz (multibeam sonar) and at 100kHz (sidescan sonar). We also made an attempt to invert the acoustic backscatter model and then obtain estimates for sediment acoustic properties and fluid/gas content. To test this approach, we used a Simrad EM300 (30kHz) multibeam sonar dataset from Skjalfandi Bay, Iceland.

The analysis starts with the backscatter time series stored in raw Simrad datagrams, which are then corrected for seafloor slope, insonification area, time varying and angle varying gains. Initially, we looked only at the angular sector between 30° and 60°. This sector is the most sensitive to volume backscatter, as in the near nadir region the backscatter is dominated by seafloor roughness and impedance contrasts. Furthermore, beyond the critical angle only a small fraction of the acoustic energy penetrates the seafloor, which makes volume scatter a secondary contribution. At the same time we used the core database to extract physical properties for the surficial sediments. These physical properties and an acoustic backscatter model were used to calculate the predicted backscatter values. The difference between the predicted (based on physical properties) and measured (with EM1000) backscatter defined a "backscatter anomaly", which showed anomalously high backscatter in deeper waters and anomalously low backscatter in shallow water. Several lines of evidence suggest an association of gas with the backscatter anomalies. In order to better understand the effect of gas on backscatter, we extended the Williams, K. L. (2001) model to include gas as a function of volume concentration and depth (Fonseca and Mayer, 2001). Through the use of 2D and 3D GIS combined with theoretical modeling we have been able to demonstrate that the surficial backscatter of the Eel River margin appears to be responding, in a complex way to gas in the sediment.

In our attempt to invert the used backscatter model, it became clear that its direct inversion was an ill-posed problem. In order overcome this limitations, we applied a constrained interactive inversion of the model, imposing constraints based on Hamilton relations for sediment physical properties, and building parametric equations with the AVO (amplitude-versus-offset) parameters calculated from the backscatter angular response. The AVO attributes (near, far, slope, gradient, fluid factor, product etc) were calculated from the stacking of a number of consecutive time series. Based on the calculated AVO attributes and the constrained inversion of the acoustic backscatter model, we estimate the gas/fluid content, the acoustic impedance and the roughness of the insonified area on the seafloor. In Skjalfandi Bay, the areas with high fluid factor anomalies correlated to regions that showed evidence of gas in seismic profiles.

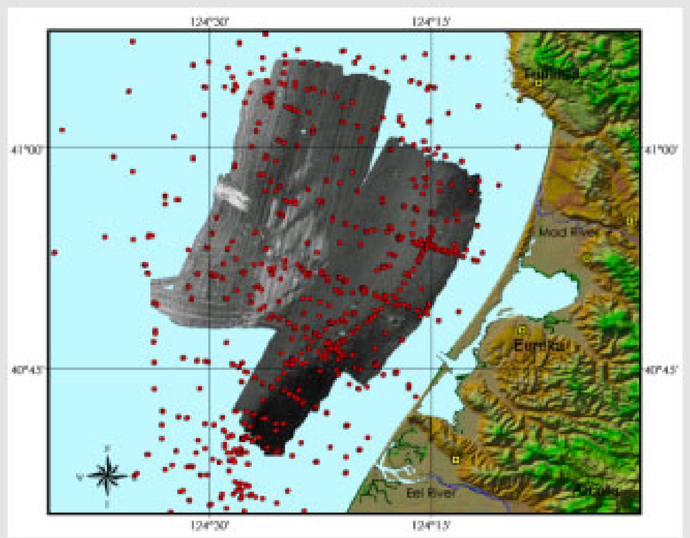

Fig. 1. Eel River Margin - Em1000 multibeam sonar survey area showing acoustic backscatter response (High backscatter in white, low backscatter in black). The red dots are core-sampling sites.

I would like to express my thanks to to Janet Yun and Dan Orange for the Eel shelf data that they provided and to Bjarni Richter for the Skjalfandi Bay analysis.

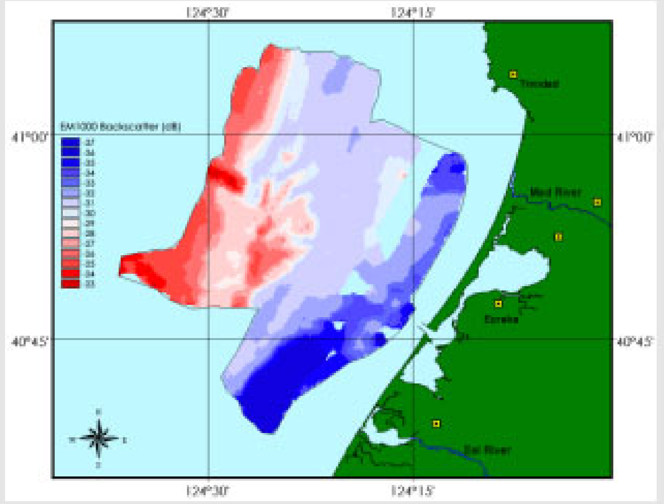

Fig. 2. The fully corrected backscatter for the Eel River Margin. Note te high backscatter in the deep waters and the low backscatter in the shallow water -- this is counter-intuitive as we would expect higher backscatter associated with the coarser grained sediments.

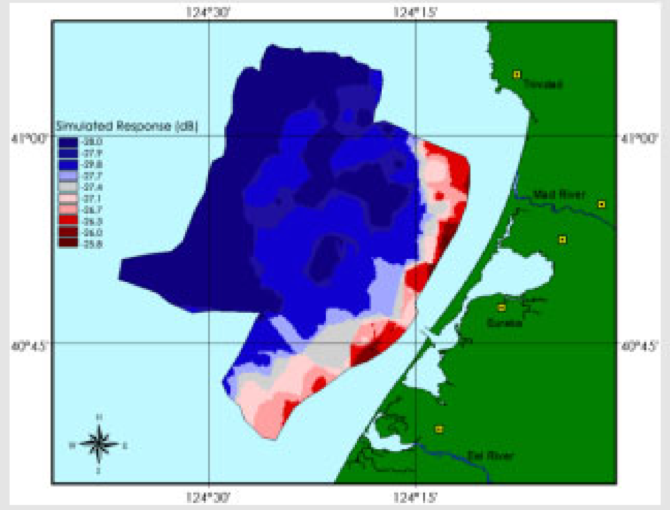

Fig. 3. Simulated backscatter response. The model predicts a higher backscatter in shallow water, where coarser high-impedance sediments are present. In deeper waters, the model predicts lower backscatter, due to the low acoustic impedance and finer grain sizes. This is in contrast to the measured backscatter.

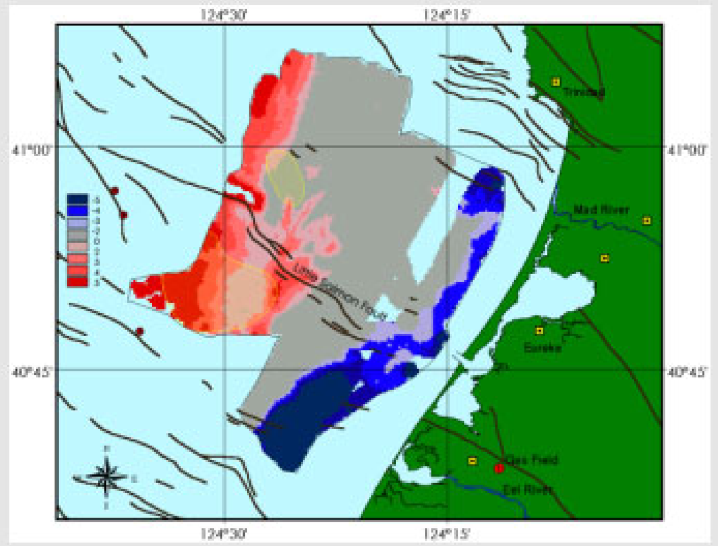

Fig. 4. Backscatter anomaly with distribution of faults. The proximity of the Little Salmon Fault can facilitate the gas migration from the reservoir to the crest of the anticline. In fact, the extension of this fault zone inland crosses a productive gas field

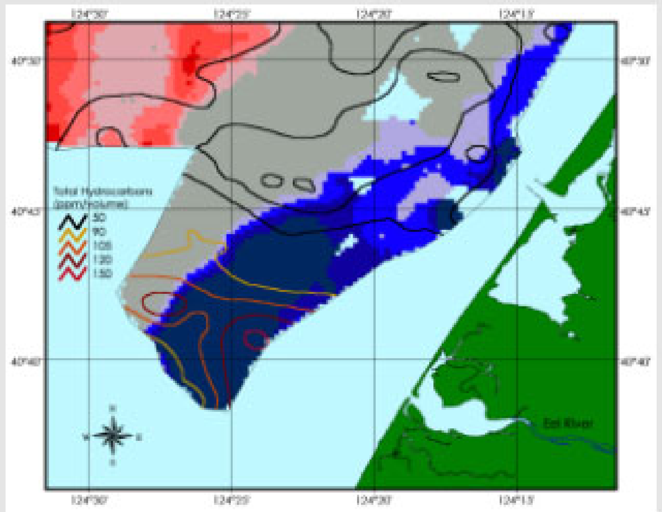

Fig. 5. A small amount of free gas on the sediment structure can explain the prominent negative backscatter anomaly on the Eel River subaqueous delta. Gas was reported on the Eel subaqueous delta based on measured geochemical anomalies using a towed gas chromatograph.

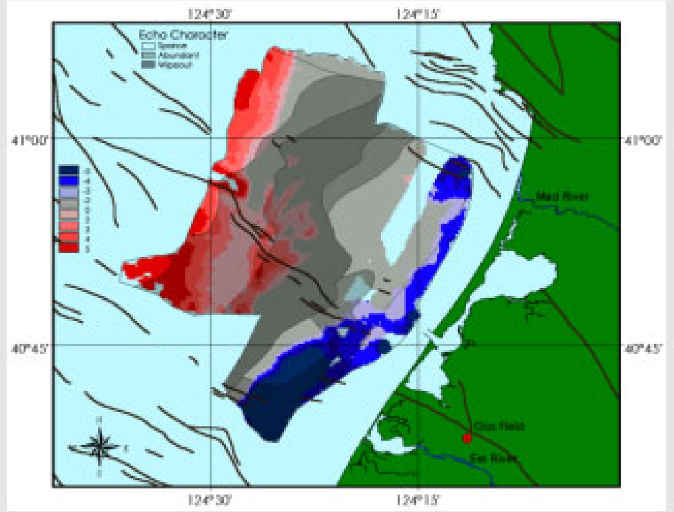

Fig. 6. Echo character map showing the distribution of subsurface gas. The presence of gas was inferred in seismic profiles based upon the presence of brightspots (abundant gas), and wipeout zones, which are acoustically transparent areas (Yun 2000). Note that the positive backscatter anomalies of the headscarp of Humbold and Northwest slides are inside a gas wipeout zone inferred from the seismic profiles

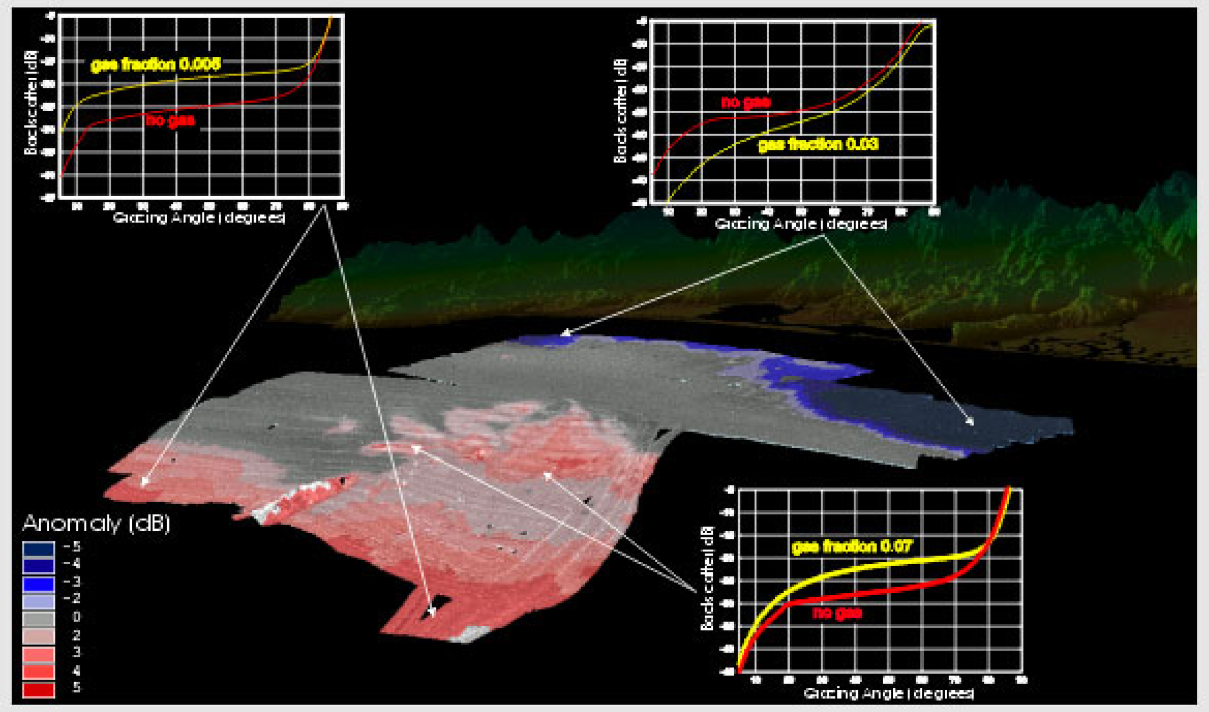

Fig. 7. The model shows that depth plays an important role in the backscatter response of gassy sediments. In deep water a small amount of gas can result in a very high backscatter, a consequence of the higher bubble stiffness at high ambient pressure. In shallow water (less than 100m), the interface backscatter is severely reduced when the sediment is charged with free gas, due to decrease of sediment sound speed. Additionally, the volume contribution in shallow water is lower, due to higher attenuation of the bubbles in lower ambient pressure. This combination of factors often results in a net decrease in the total backscatter response in shallow water, relative to a gas-free sediment with the same physical properties.

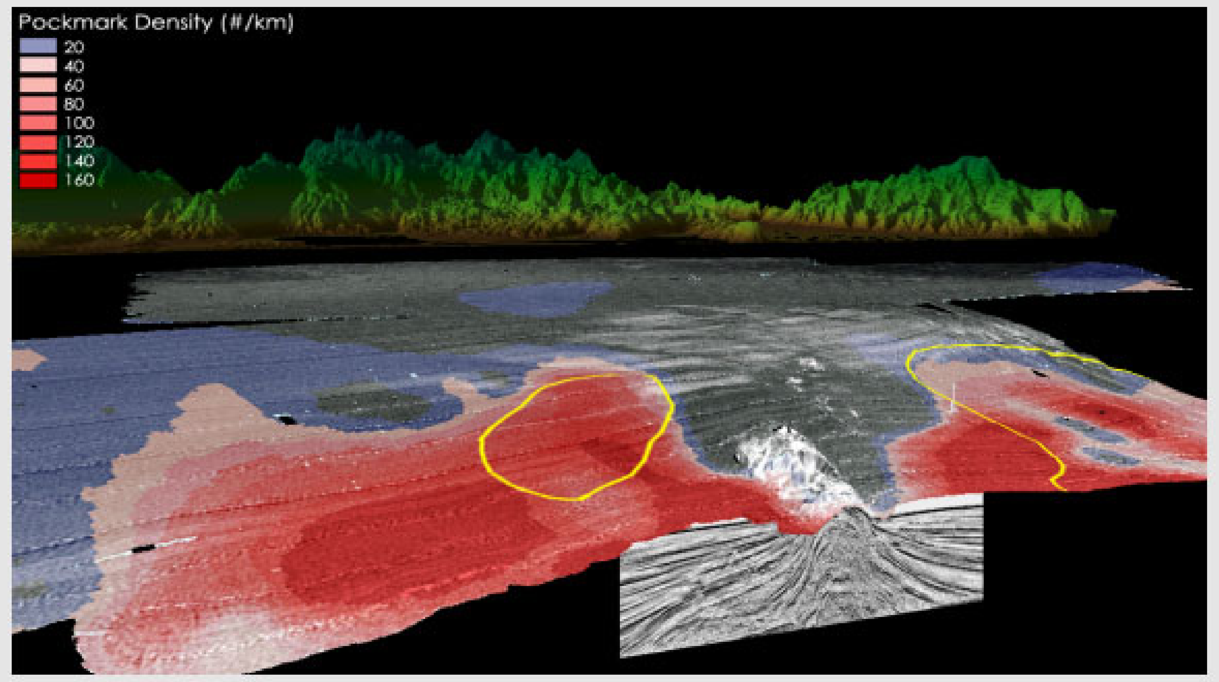

Fig. 8.. Density of pockmarks determined from deep-towed sidescan sonar with areas of landslide (yellow polygons). The positive backscatter anomaly associated to the high concentration of pockmarks in water depths beyond 400m suggests the presence of active seeping gas in this part of the survey area. The gas probably comes from the dissociation of hydrates, which were indicated in these areas by the presence of bottom-simulating reflections in high-resolution seismic lines (Yun, 1999). There is evidence that the near-surface gas on the headscarps of Humboldt and Northwest slides may come from deep reservoir sources. Gas probably accumulates at the impermeable crest of this anticline until it seeps to the surface through factures at the base of the folded structure. This seeping gas can explain the positive backscatter anomalies around the folded structure

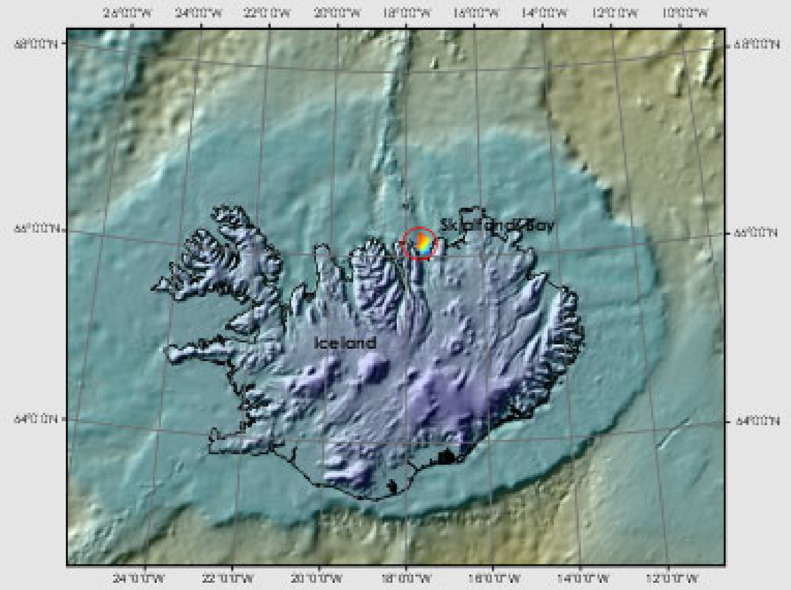

Fig. 9. The inversion based on AVO analysis was applied to one acoustic remote sensing dataset acquired in the summer of 2003 in Skjalfandi Bay, Iceland. The equipment used was a Simrad EM300 multibeam sonar, a shallow water system operating at 30KHz, forming 135 beams in an angular sector of 150 degrees. The survey also included a Subscan SB0512 high-frequency seismic profiler (chirp sonar) and a tow-cam unit for bottom photographs. The survey mapped water depths from 50 to 230m, in an area covered with fluid expulsion features (pockmarks).

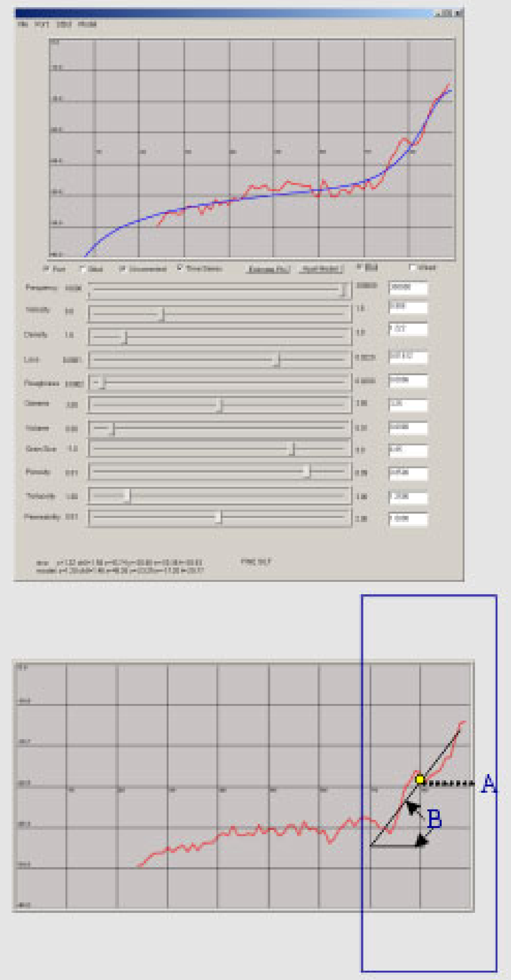

Fig. 10. The AVO parameters preserve some information form the angular signature. For that, the near soundings, i.e. the soundings with incident angle closer to the nadir, will be processed separately from the far sounding, i.e., the sounding with shallow incident angles. Additionally, the slope and the intercept of the angular response curve are calculated. The slope is basically controlled by the roughness, while the intercept is controlled by the impedance, although the actual relationship is complex and is described the mathematical model for the acoustic backscatter.

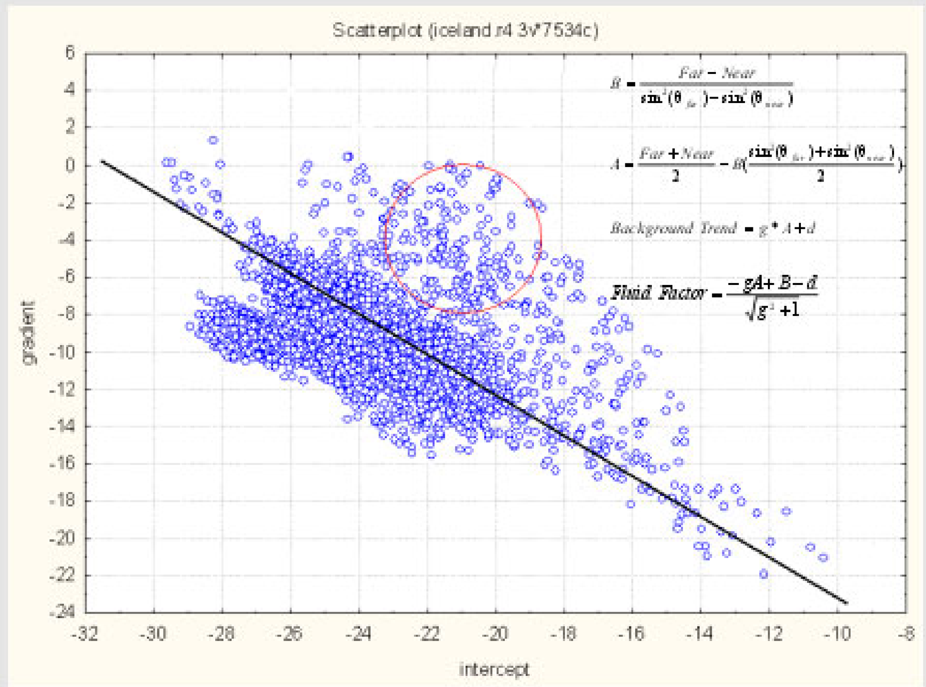

Fig. 11. One important AVO parameter used to characterize the backscatter angular response is the Fluid-Factor. According to the backscatter modeling, this attribute is directly related to the amount of free fluid, normally gas, in the sediment structure. Initially, the background trend line for the survey is defined as the linear regression of all coordinate pairs (slope, intercept) in the slope-intercept plane. Then, the fluid factor attribute is defined as the orthogonal distance of each coordinate pair to the background trend.

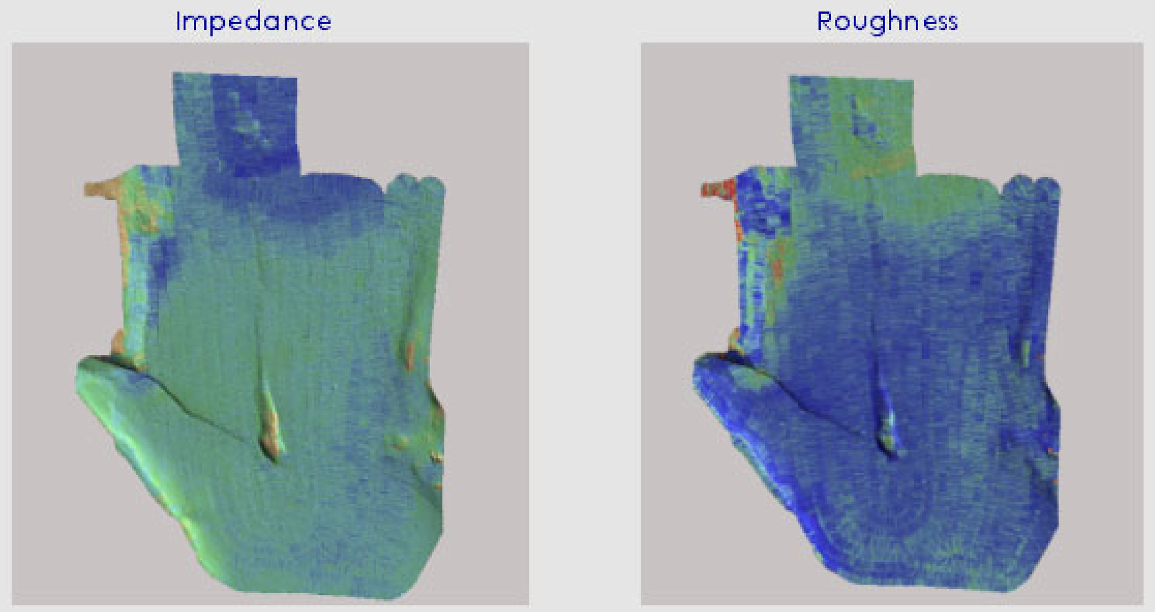

Fig. 12. Based on the calculated AVO attributes (near, far, slope, gradient, fluid factor, product etc) and the inversion of the acoustic backscatter model, we estimate the acoustic impedance and the roughness of the insonified area on the seafloor.

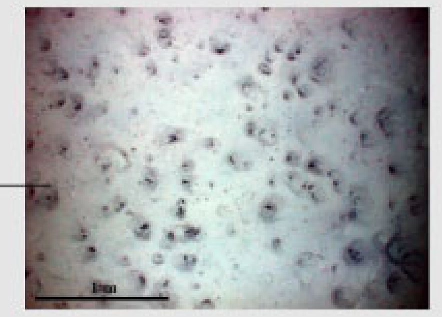

Fig. 13. Bottom photographs show abundant holes within some large pockmarks that are evidence of water/gas expulsion. Few amplitude anomalies are seen in the chirp profiles, which seem to indicate that most of the pockmarks are inactive at the moment, as they show sediment infill.

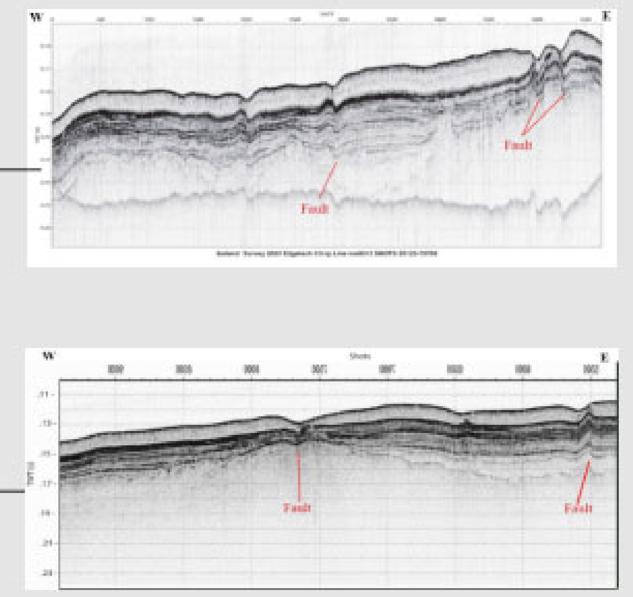

Fig. 14. High amplitude anomalies in the chip profiles are evidence of gas seepages and active pockmarks. Most of the pockmarks seem to be connected to underlying N-S trending faults and show disturbance of the sediment beneath and no infill, a clear indication that they are still active.

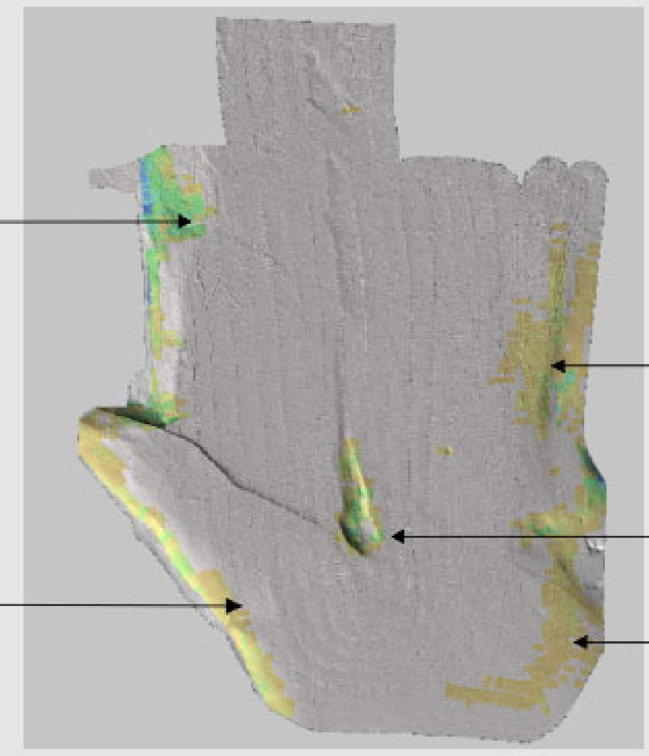

Fig. 15. Map of Fluid Factor anomaly in Skjalfandi Bay. Areas of High negative anomalies indicate the presence of free fluid/gas in the shallow sediments structure. These areas correlated to regions that showed evidence of gas in seismic profiles and bottom photographs.

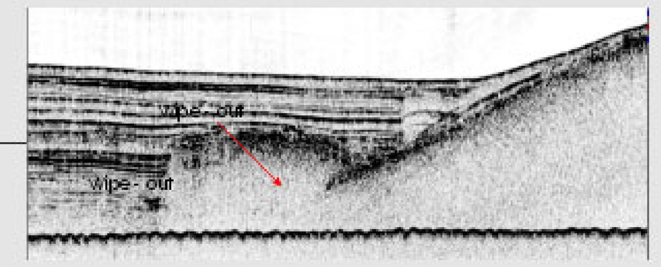

Fig. 16. Acoustic transparent areas (wipe-out zones) in the chirp profiles are a clear evidence of the presence of highly gas-charged sediments in the subsurface.

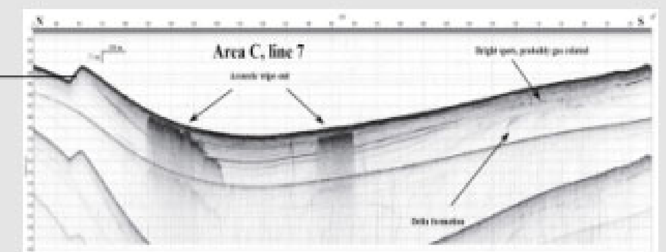

Fig. 17. Acoustic transparent areas in the chirp profiles are a clear evidence of the presence of highly gas-charged sediments in the subsurface.

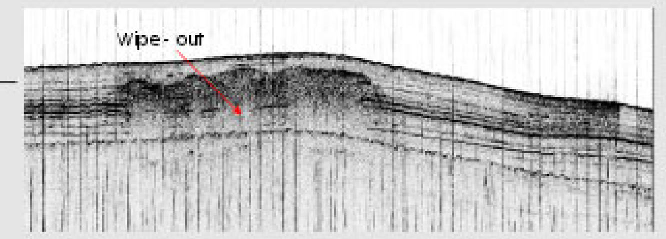

Fig. 18. Acoustic transparent areas in the chirp profiles are a clear evidence of the presence of highly gas-charged sediments in the subsurface.

Center for Coastal and Ocean Mapping
University of New Hampshire
[1]luciano@ccom.unh.edu
[2]lmayer@unh.edu